- Technical Paper -

PERFORMANCE OF CONFINED BOUNDARY REGIONS OF RC RECTANGULAR WALLS UNDER CYCLIC REVERSAL LOADINGS

Rafik TALEB[*1], Masaya OGURA[*2], Susumu KONO[*3], and Masanori TANI[*4]

ABSTRACT

In order to investigate effects of reinforcement detailing, slenderness and loading history on the capacity and failure modes of confined boundary regions of RC rectangular structural walls, eight RC rectangular element specimens were tested under monotonic and cyclic reversal loadings. It was found that the tensile strain prior to compressive strain affected the failure mode and maximum capacity of thin wall boundaries.

Keywords: RC structural walls, confined boundary region, confinement, buckling failure.

1. INTRODUCTION

Reinforced concrete structural walls are commonly used as lateral-load resisting components in multi-story building structures. When well designed and detailed, walls are considered to perform well under earthquake loading. Observed damages of RC wall buildings in recent earthquakes in Chile and New Zealand raised, however, concern about the seismic performance of rectangular RC walls. In these earthquakes, severe damage happened to concrete walls in numerous walled buildings leading to partial or total collapse. Structural wall damage of boundary regions, such as spalling and crushing of concrete, often spread over the wall length. Longitudinal reinforcement in this region fractured under tension or buckled under compression. Sometimes global wall buckling was observed. It was reported that lack of adequate confinement and detailing in boundary regions was one of the main causes of those damages. It is considered that more studies are needed to clarify their seismic performance. These types of damage raise questions about the mechanisms that lead to reinforcing bars buckling, concrete crushing, and global wall buckling. In particular, the quantity and configuration of transverse reinforcement required at wall boundaries needs to be reassessed. It is considered that failure mechanisms are affected by wall thickness, slenderness, axial load level, and section configuration, as well as displacement and load history. Preliminary studies indicated that greater amounts of transverse reinforcement may be required for thin walls and that tighter spacing of transverse reinforcement may be required to suppress buckling of vertical reinforcement [1, 2]. However, there is no integrated theory to explain wall damage and failure under seismic loading. It is worth to mention that the AIJ Standard for Structural Calculations of Reinforced Concrete Buildings [3] was revised in 2010 to allow the use of RC walls with rectangular cross-sections, although the use of walls with boundary columns is still the common practice in Japan.

In order to clarify the influence of reinforcement detailing, slenderness and loading history on the capacity and failure modes of confined boundary regions of RC rectangular structural walls, eight RC rectangular element specimens were tested and damage process was studied.

2. EXPERIMENTAL PROGRAM

An experimental program was conducted in order to bring insight on the seismic performance of confined boundaries of RC rectangular walls. The objective was to investigate the influence of longitudinal and transverse reinforcement amount, slenderness and load history (Monotonic and cyclic) on their capacity, damage process and failure modes. The boundary regions of the wall were idealized as an axially loaded rectangular RC column. Although the approach does not account for the strain gradient expected across the section, the idealization is useful in providing an understanding of the mechanism involved during lateral loading of the RC wall.

2.1. Description of Test Specimens

Table 1 shows cross-sectional configurations and reinforcement layouts of the tested elements. Eight rectangular elements with two different sectional dimensions (B-type and C-type) having approximately similar cross-sectional area were constructed and tested. The element specimens were built without cover concrete so that the intermediate damage state due to spalling of cover concrete could be eliminated, since the objective was to assess ultimate behavior and

*1 Doctoral student, Dept. of Environmental Science and Technology, Tokyo Institute of Technology, JCI Member
*2 Graduate Student, Dept. of Environmental Science and Technology, Tokyo Institute of Technology, JCI Member
*3 Professor, Materials and Structures Laboratory, Tokyo Institute of Technology, JCI Member
*4 Research Engineer, Building Research Institute, Tsukuba, JCI Member

failure modes. The cross sections were 112×242 mm^2 and 72×367 mm^2 for B-type and C-type elements, respectively, representing two levels of slenderness. The dimensions are measured from centerline to centerline of extreme transverse reinforcing bars. The shorter side length of the section corresponds to wall thickness. For each sectional type, two levels of transverse reinforcement were set. Four configurations were replicated in order that each configuration is tested under monotonic compression loading and cyclic reversal loading. The last character in the specimen labels stands for loading type: M for monotonic and C for cyclic.

Table 2 shows the amounts of longitudinal and transversal reinforcement as well as loading type for each element specimen. D4 (SD295A) deformed reinforcing bars were used for transverse reinforcement for lightly confined specimens with 80 mm and 70 mm spacing for 5B and 1C elements, respectively, and D6 (SD295A) for densely confined specimens with 80 mm and 40 mm spacing for 6B and 3C elements, respectively. 5B and 1C specimen types were designed to have similar transverse reinforcement ratio. All transverse reinforcement had 135-degree hooks. D16 (SD295A) and D10 (SD295A) deformed reinforcing bars were used for longitudinal reinforcement for B-type (p_g = 7.33%) and C-type (p_g = 3.24%) elements, respectively. Figure 1 shows vertical reinforcement layout of 6B elements configuration. Longitudinal reinforcing bars of elements were bent 180-degrees at their ends and hanged to a D25 (SD345) deformed reinforcing bars in the upper and lower stub to ensure fixity. D25 bars were also used as longitudinal reinforcement for lower and upper stub and D10 was used for transverse reinforcement. The tested elements had 600 mm height with fix-ended at both ends. This height represents the lower portion of the confined boundary in a wall where likely compressive failure may occur. Previous experimental studies indicate that the compressive failure region is quite limited within a height of about 2.5 times the wall thickness [4, 5]. The elements were cast in two stages: first the lower stub and then the element and the upper stub as one part with intentionally roughened surface created at lower stub–element interface to insure adherence.

Table 1 Cross-sections and reinforcement details

	Light confinement	Dense confinement
Label	5B-M & 5B-C	6B-M & 6B-C
B-Type	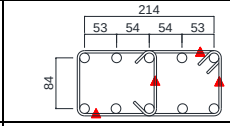	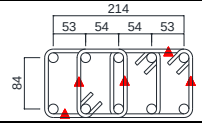
Label	1C-M & 1C-C	3C-M & 3C-C
C-Type	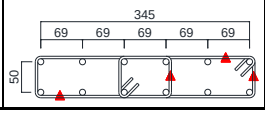	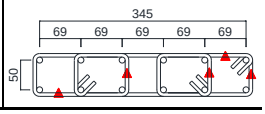

Table 2 Reinforcement amount and loading type

Specimen	Long. Reinf	Transv. Reinf.	Loading
5B-M	10-D16 (p_g = 7.33%)	3-D4@80 (p_w = 0.22%)	Monotonic
5B-C			Cyclic
6B-M		6-D6@80 (p_w = 0.98%)	Monotonic
6B-C			Cyclic
1C-M	12-D10 (p_g = 3.24%)	4-D4@70 (p_w = 0.22%)	Monotonic
1C-C			Cyclic
3C-M		6-D6@40 (p_w = 1.29%)	Monotonic
3C-C			Cyclic

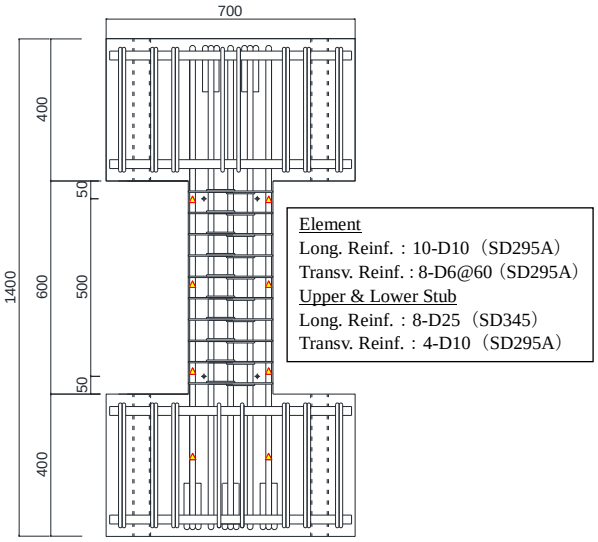

Fig. 1 Vertical reinforcement layout of 6B-M and 6B-C specimens

Table 3 and Table 4 show measured material properties for concrete and reinforcing bars, respectively. A concrete mix with 13 mm of maximum aggregate size and 18 cm for slump test were used.

Table 3 Concrete mechanical properties

Compressive strength (MPa)	Strain at peak (%)	Young's modulus (GPa)	Splitting strength (MPa)
24.5	0.18	26.3	2.3

Table 4 Reinforcing bars mechanical properties

bars	Yield strength (MPa)	Ultimate strength (MPa)	Young's modulus (GPa)
D4	363	532	/
D6	365	516	192
D10	347	484	190
D16	325	462	188
D25	381	567	192

2.2. Loading Method

A universal testing machine was used to apply vertical load on the upper stub under the condition of uniaxial tension and compression (Figure 2). For monotonic tests, the axial compression load was

applied gradually until failure. For cyclic tests, axial loading history was determined based on the average strain at the lower part of previously tested RC structural walls [6]. The loading cycle consisted of an initial half-cycle of axial tensile strain followed by a compression half cycle with a nominal target compressive strain 1/5 of the axial tensile strain, unless the compression cycle was limited by the capacity of the loading machine which was 1500 kN. Thus, two cycles of loading were applied that correspond to yielding strain followed by tensile strains, ε_t, of 0.5%, 1%, 1.5% 2% 2.5%, 3% and 4% for B-type elements and tensile strains, ε_t, of 0.75%, 1.5%, 2%, 3% and 4% for C-type elements as shown in Figure 2.

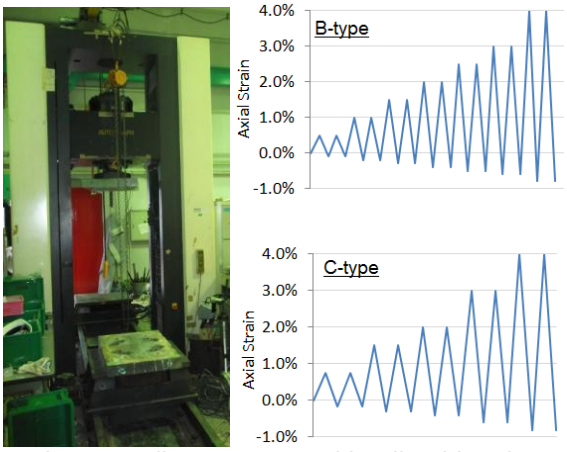

Fig. 2 Loading system and loading histories

2.3. Measurement

Displacement transducers were mounted to both ends of the longer side length of the section at intervals of 0~50 mm (Z1), 50~550 mm (Z2) and 550~600 mm (Z3) for B-type elements, and at intervals of 0~40 mm (Z1), 40~560 mm (Z2) and 560~600 mm (Z3) for C-type elements. Two displacement transducers were also installed between upper and lower stub at both sides. Experimentally, the nominal axial strain was defined as the strain corresponding to average displacement at both ends of the element over the total height.

3. EXPERIMENTAL RESULTS AND DISCUSSION

3.1. Damage process and failure modes

Photo 1 shows the final damage of all specimens. Damage evolution and failure modes are described for each configuration in the following paragraphs.

5B-C and 5B-M elements: For 5B-C element, horizontal cracks appeared uniformly at transverse reinforcement planes when loading in tension, indicating that these cracks were initiated by the transverse reinforcement. At further tensile strain, horizontal cracks opened widely and new horizontal cracks formed at mid-spacing between transverse reinforcement. At final stage, buckling of multiple longitudinal reinforcing bars happened simultaneously at mid-height region of the element over two or three spacing of transverse reinforcement. Buckling of longitudinal reinforcement was followed by crushing of concrete in buckling region. Buckling of unsupported intermediate bars was more pronounced compared to other bars. 5B-M element under monotonic loading reached maximum capacity without visible damage, followed by spalling of concrete and buckling of longitudinal reinforcement over three transverse reinforcement spacing similarly to 5B-C specimen.

6B-C and 6B-M elements: For 6B-C element, horizontal cracks appeared at transverse reinforcement planes under tension loading. Cracks opened widely as tensile strains increased. At final loading stage, both 6B-C and 6B-M elements failed by crushing of compressive concrete followed by localized buckling of the damaged region. The damaged region was located at the lower portion of for 6B-M and at the top for 6B-C.

1C-C and 1C-M elements: For 1C-C element, horizontal cracks appeared at transverse reinforcement planes under tension loading. Under compression, both elements failed by buckling of longitudinal reinforcement. Buckling was observed over two and three transverse reinforcement spacing for 1C-M tested under monotonic loading, while buckling length extended over more than four spacing due to pre-cracks induced by tensile strain. Pre-cracking condition facilitate the buckling of longitudinal reinforcement. Similarly to 5B elements, buckling of unsupported intermediate bars was more pronounced than other bars, suggesting that restraining unsupported intermediate bars in the confined boundary region should be considered.

3C-C and 3C-M elements: Similarly, horizontal cracks appeared at transverse reinforcement planes for 3C-C element under tension loading. Final failure for 3C-M element was due to extensive crushing of compressive concrete at the bottom of element over a very limited height (about two transverse reinforcement spacing). Crushing of concrete for 3C-C element was also concentrated at the bottom within limited height, similarly to 3C-M. However, crushing of concrete in 3C-C was followed by global buckling of the element when unloading from the second cycle of 4% tensile strain. This indicates that global buckling was driven by prior induced large tensile strain which demonstrates the vulnerability of confined boundaries of slender walls to tensile strain excursions prior to compressive strain. Spread of concrete crushing was limited in height compared to B-type elements.

Globally, no difference of the failure modes were shown when comparing failures under monotonic and cyclic loading condition. Exception was noted for 3C-M and 3C-C elements representing boundaries of slender rectangular walls where extensive and concentrated concrete crushing happened at the element base. Crushing of concrete at the base of 3C-C was followed by global buckling of the element. This prior crushing assisted the global buckling to happen over almost the total height of the element and resulted in a large out-of-plan displacement.

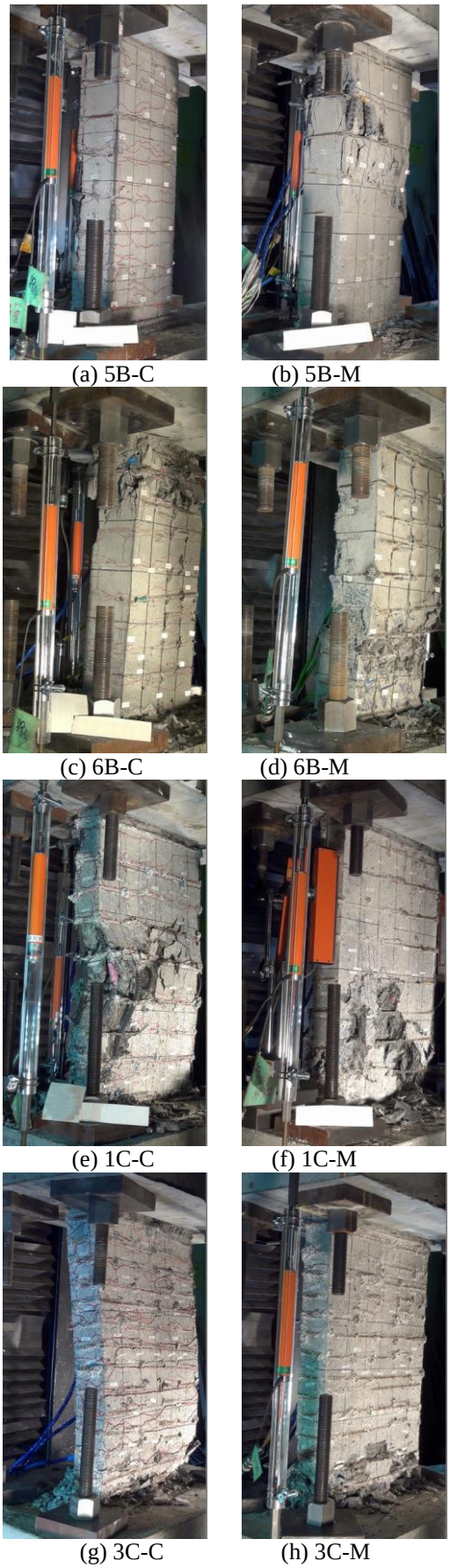

(a) 5B-C (b) 5B-M

(c) 6B-C (d) 6B-M

(e) 1C-C (f) 1C-M

(g) 3C-C (h) 3C-M

Photo 1 Final damage situation

Photo 2 shows the final buckled shape of the 3C-C element. A vertical broken line was drawn to highlight the transverse curvature of the buckled element in the figure. Wide cracks developed at transverse reinforcement planes as a result of a large yield excursion and did not close prior to full development of maximum axial strength in the reversed direction. This damage situation caused a critical condition affecting the lateral stability of the wall as this phenomenon had been previously studied [7, 8]. However, buckling pattern indicates that previously crushed region contributed in a large out-of-plan displacement. This reveals that both large axial strain prior to compressive strain and prior crushing affect the global buckling failure mode for slender walls. Imposing a minimum wall thickness would be an alternative means to suppress failures due to global buckling.

The lack of closely spaced transverse reinforcement and/or thin core concrete for elements failed due to buckling of longitudinal reinforcement, a stable compression zone could not be sustained and spread of concrete crushing by confined core concrete could not be ensured.

Photo 2 Final buckled shape of 3C-C specimen

3.2. Axial load-Axial nominal strain relationships

Figure 3 shows axial load versus axial nominal strain relationships. The red and blue broken lines indicate, respectively, the calculated loads corresponding to the yielding of longitudinal reinforcements and compressive strength as sum of the concrete uniaxial strength and yield stress of longitudinal reinforcement. Damage characteristic points are also shown corresponding to longitudinal reinforcement compressive yielding, transverse reinforcement yielding, compressive capacity, onset of longitudinal reinforcement buckling and global element buckling. Table 5 reports load and strain levels for considered damage characteristic point as well as maximum tensile strain for each specimen. It should be noted that excessively large compressive strain for 6B elements was due to a rotation of the elements prior to extensive crushing.

Under low levels of axial tensile strain for element tested under cyclic loading, a stable response was obtained. However, increasing the tensile strain level led to different response. These differences and the comparison of monotonic and cyclic loading response are summarized in the following.

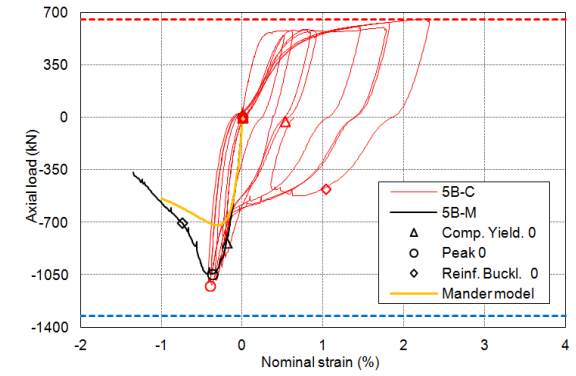

(a) 5B-C & 5B-M

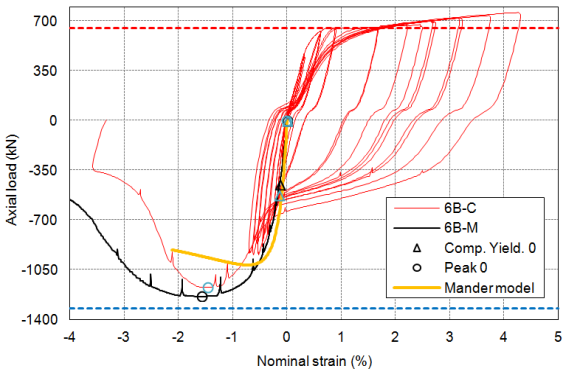

(b) 6B-C & 6B-M

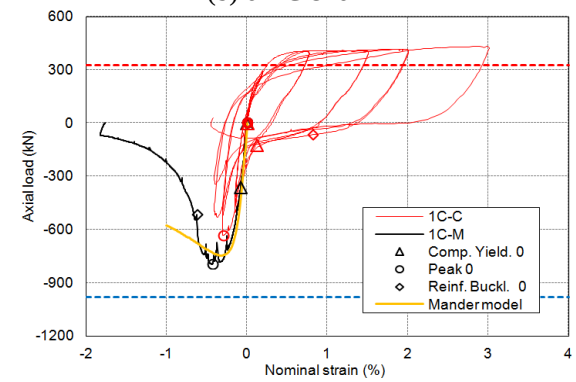

(c) 1C-C & 1C-M

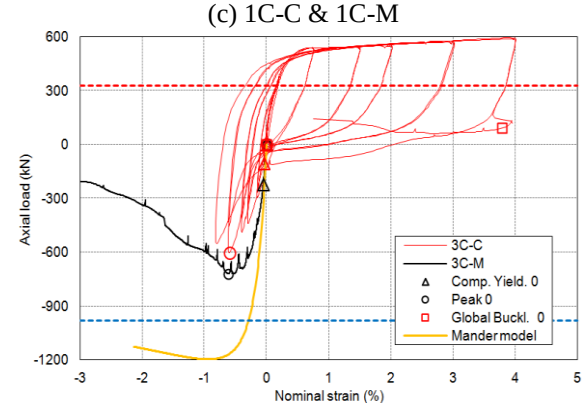

(d) 3C-C & 3C-M

Fig. 3 Axial load-Nominal axial strain relationships

Comparison of capacity between monotonic and cyclic loadings showed no significant difference for B-Type elements. However, capacity reduced for C-type elements under cyclic loading by approximately 18% of that under monotonic loading. The capacity difference was more significant for elements that failed due to longitudinal reinforcement buckling (5B and 1C specimens). After reaching the maximum capacity, element 1C-C showed the most drastic reduction of load capacity after reaching the compression peak load at first cycle of 1.5% tensile strain. The capacity reduced from -635 kN at peak point to -524 kN at second cycle of 1.5% tensile strain, and continued to decrease from -526 kN to -337 kN between first and second cycle of loading corresponding to 2% tensile strain. However, the compressive capacity drop was not so high in comparison to previous research [9] where a reduction of more than two third of the capacity was shown when comparing element under direct compression test and that subjected to tension strain of 4% prior to compression. The difference of final failure mode was also reported between the two loading methods.

Comparison between monotonic and cyclic response for elements that failed due to buckling of longitudinal reinforcement (5B and 1C) shows that prior tensile strain affects considerably the onset of longitudinal reinforcement buckling. Onset of buckling was noted at load levels of -701 kN and -477 kN for 5B-M and 5B-C, respectively (32% reduction), and at -518 kN and -66 kN for 1C-M and 1C-C, respectively (87% reduction). All buckling of longitudinal reinforcement occurred after bars have yielded in compression. For both elements tested under cyclic loading, buckling of reinforcement happened when unloading from tensile side and loading to the corresponding compression strain. Reinforcement buckling for 5B-C happened at smaller tensile strain cycle (2.5%) compared to 1C-C (3%). This is probably due to large transverse reinforcement spacing that is likely to result in buckling of longitudinal reinforcement following even limited tensile strain excursions. Response curves of 5B and 1C that failed by buckling of longitudinal reinforcement showed a quick decrease of axial load after the peak compressive load was reached.

Table 5 Damage characteristic points

Elem.	Reinf. Comp. yield. (kN)	Trans. Reinf. yield. (kN)	Peak Point (kN)	Long. Reinf. Buckl (kN).	Glob. Buckl. (kN)	Max tens. Strain (%)
5B-M	-834.2 (-0.20)	-1004 (-0.38)	-1045 (-0.38)	-701 (-0.75)	/	/
5B-C	-23.6 (0.53)	-523 (1.09)	-1121 (-0.40)	-477 (1.03)	/	2.3
6B-M	-453 (-0.14)	-1125 (-0.77)	-1237 (-1.58)	/	/	/
6B-C	-528 (-0.15)	-1046 (-0.91)	-1175 (-1.47)	/	/	4.3
1C-M	-361 (-0.08)	-790 (-0.43)	-795 (-0.44)	-518 (-0.63)	/	/
1C-C	-123 (0.11)	-606 (-0.22)	-635 (-0.3)	-66 (0.88)	/	3
3C-M	-223 (-0.06)	-687 (-0.40)	-719 (-0.62)	/	/	/
3C-C	-106 (-0.04)	-340 (-0.20)	-604 (-0.60)	/	95	4

The value in ( ) is the corresponding nominal strain in % at the specified damage state.

Comparing densely and lightly confined specimens, it was shown that well confined specimens revealed capability to sustain larger tensile strain in a stable manner. However, dense transverse reinforcement detailing added little to the capacity of the B-type elements. For C-type elements and although 3C elements were highly confined than 1C element, the compressive capacity of 1C elements were higher than that of 3C under both monotonic and cyclic loading. This could be attributed to honeycombs that appeared at the base of 3C elements due to slenderness (80mm thickness) and close spacing of transverse reinforcement (40mm) that also led to damage concentration at the base of the elements.

These observations suggest that it may not be even possible to provide enough confinement in thin sections by close transverse reinforcement spacing because the core concrete area is small and the pattern of concrete crushing indicated that compression strain concentrates over a short height. Thus moderate amounts of well-detailed confinement may not improve performance.

4. PREDICTION OF AXIAL LOAD-AXIAL STRAIN RELATION AND BUCKLING STRAIN

Predictions of the axial load-axial strain relationships under monotonic load using the well-known Mander model [10] are shown on Figure 3 along with experimental curves. The model highly overestimated the maximum load for 1C specimens which reflect that high confinement could not be effective because the core concrete area was small.

Longitudinal reinforcement buckling length and buckling strain was predicted using Kato model [11] for 5B-M and 1C-M specimens that failed by buckling of longitudinal reinforcement under monotonic loading. The predicted buckling length agreed with experimental observation. However, buckling strains resulted in non conservative predictions. Predicted buckling strains were 3.70% and 7.67% for 5B-M and 1C-M, respectively, while were 0.86% and 2.67% for test conditions.

5. CONCLUSIONS

The following conclusions can be drawn.

(1) Three different failure modes were observed depending on confinement and slenderness levels: crushing of compressive concrete, buckling of longitudinal reinforcement, and global buckling of element.

(2) Dense transverse reinforcement detailing in thin confined boundaries is not efficient to improve the performance of walls. Imposing a minimum wall thickness would be an alternative means to suppress failures due to global buckling of thin walls.

(3) Failure due to global buckling is affected by both large axial strains prior to compressive strain and prior crushing of compressive concrete.

(4) Large transverse reinforcement spacing may result in buckling of longitudinal reinforcement following even limited tensile strain excursions. Design criterion for longitudinal reinforcement buckling should be considered.

(5) Large spacing between adjacent hoops or ties does not provide sufficient confinement. A limit should be considered at the same level with the limit of transverse reinforcement spacing to improve confinement.

ACKNOWLEDGEMENT

The authors gratefully acknowledge the financial support of the Ministry of Land, Infrastructure, Transportation and Tourism (Japan).

REFERENCES

[1] Talleen K, Maffei J, Heintz J, Dragovich J. Practical Lessons for Concrete Wall Design Based on Studies of the 2010 Chile Earthquake. Proceedings of the 15th WCEE, Portugal, 2012.

[2] Wallace JW. Performance of Structural Walls in Recent Earthquakes and Tests and Implication for US Building Codes. Proceedings of the 15th WCEE, Portugal, 2012.

[3] Architectural Institute of Japan. AIJ Standard for Structural Calculation of Reinforced Concrete Structures, Tokyo, Japan, 2010. (in Japanese)

[4] Markeset G, Hillerborg A. Softening of Concrete Compression Localization and Size Effects. Cement and Concrete Research 1995. 25(4): 702-708.

[5] Takahashi K. et *al.* Flexural Drift Capacity of Reinforced Concrete Wall with Limited Confinement. ACI Structural Journal, 110(1): 95-104.

[6] Toya K, Ogura M, Tani M, Kono S. Effects of confined and region and axial load on the flexural ultrmate deformation of RC walls without boundary columns, JCI 2013 Convention, Nagoya, Japan, 6p. (in Japanese)

[7] Paulay T, Priestley M.J.N. Stability of Ductile Structural Walls. ACI Structural Journal 1993, 90-S41: 385-392.

[8] Chai YH, Elayer DT. Lateral Stability of Reinforced Concrete Columns under Axial Reversed Cyclic Tension and Compression, ACI Structural Journal 1999, 96(5): 780-789.

[9] A. Creagh, et al. Seismic Performance of Concrete Special Boundary Element, NEESreu Program Summer 2010, pp.1-18, 2010.

[10] Mander JB, Priestley MJN, Park R. Theoretical Stress-Strain Model for Confined Concrete. ASCE Journal of Structural Engineering 1988, 114(8): 1804-1825.

[11] Kato D. Buckling Behaviors of Steel Bars in R/C Columns. Journal of Struct. Constr. Eng., AIJ 1992, 436: 135-143. (in Japanese)